BJP BRITISH JOURNAL OF PHARMACOLOGY

BPS BRITISH PHARMACOLOGICAL SOCIETY

British Journal of Pharmacology (2010), 160, 1338–1351
© 2010 The Author
Journal compilation © 2010 The British Pharmacological Society All rights reserved
0007-1188/10
www.brjpharmacol.org

RESEARCH PAPER

Acurhagin-C, an ECD disintegrin, inhibits integrin αvβ3-mediated human endothelial cell functions by inducing apoptosis via caspase-3 activation

Wen-Jeng Wang

Department of Nutrition and Health Sciences, Chang-Gung Institute of Technology, Kwei-Shan, Tao-Yuan, Taiwan

Background and purpose: Acurhagin, a member of versatile metalloproteinase disintegrins from *Agkistrodon acutus* venom, has been identified as a platelet aggregation inhibitor, previously. Here, acurhagin-C, the C-terminal Glu-Cys-Asp (ECD)-containing fragment of acurhagin, was evaluated for its biological activities and potential applications in anti-angiogenic therapy.

Experimental approach: Human umbilical vein endothelial cells (HUVECs) were treated with acurhagin-C to assay effects on viability, apoptosis, adhesion, migration, invasion, proliferation and angiogenesis. The recognition site and signalling involved for the interactions of acurhagin-C with HUVEC were determined using flow cytometric, electrophoresis and immunoblotting analyses.

Key results: Acurhagin-C decreased viability and induced apoptosis in HUVEC. It also dose-dependently inhibited HUVEC adhesion to immobilized extracellular matrices fibronectin, collagen I and vitronectin with respective IC_{50} values of approximately 0.6, 0.3 and 0.1 μM. Acurhagin-C prevented migration and invasion of HUVEC through vitronectin- and Matrigel-coated barriers respectively. Furthermore, acurhagin-C attenuated fibroblast growth factor-2-primed angiogenesis both *in vitro* and *in vivo*, and specifically blocked the binding of anti-αvβ3 monoclonal antibody 23C6 to HUVEC in an ECD-dependent manner. However, purified αvβ3 also dose-dependently bound to immobilized acurhagin and acurhagin-C with a saturable pattern. Interference with integrin αvβ3-mediated functions and promotion of caspase-3 activation by acurhagin-C affected morphology of HUVEC and induced apoptosis.

Conclusions and implications: Acurhagin-C elicited endothelial anoikis via disruption of αvβ3/focal adhesion kinase/phosphatidylinositol 3-kinase/Akt survival cascade and subsequent initiation of the procaspase-3 apoptotic signalling pathway.
British Journal of Pharmacology (2010) **160,** 1338–1351; doi:10.1111/j.1476-5381.2010.00781.x

Keywords: acurhagin-C; *Agkistrodon acutus*; angiogenesis; Arg-Gly-Asp; apoptosis; integrin αvβ3; Glu-Cys-Asp

Abbreviations: ADAMs, disintegrin and metalloproteinase proteins; CAM, chick chorioallantoic membrane; ECD, Glu-Cys-Asp; ECM, extracellular matrix; ERK, extracellular signal-regulated kinase; FAK, focal adhesion kinase; FBS, fetal bovine serum; FITC, fluorescein isothiocyanate; FGF2, fibroblast growth factor-2; GP, glycoprotein; HRP, horseradish peroxidase; HUVECs, human umbilical vein endothelial cells; MDC, metalloproteinase/disintegrin-like/cysteine-rich; MFI, mean fluorescence intensity; MTT, 3-[4, 5-dimethylthiazol-2-yl]-2, 5-diphenyl tetrazolium bromide; P-III, protein class III; PARP, poly(ADP-ribose) polymerase; PI3K, phosphatidylinositol 3-kinase; RGD, Arg-Gly-Asp; SVMPs, snake venom metalloproteinases

Introduction

The integrins, a superfamily of adhesion molecules comprised of heterodimeric α- and β-subunits, are known to be involved in the complex processes required for cell proliferation, migration and differentiation (Danen, 2005). It has become evident that integrin αvβ3-mediated adhesion to extracellular matrix (ECM) is essential for endothelial cell growth and survival, whereas αvβ3 antagonism may induce endothelial apoptosis during angiogenesis (Erdreich-Epstein *et al*., 2005).

The disintegrins are a family of low molecular mass, cysteine-rich, naturally occurring polypeptides from a variety of *Viperidae* and *Crotalidae* snake venoms and initially described as potent inhibitors of integrin αIIbβ3 through the blockade of fibrinogen and von Willebrand factor binding to activated platelets (Marcinkiewicz, 2005). According to the

Correspondence: Professor Wen-Jeng Wang, Chang-Gung Institute of Technology, Room A810, no. 261 Wen-Hwa 1st Road, Kwei-Shan, Tao-Yuan 33303, Taiwan. E-mail: wjwang@gw.cgit.edu.tw
Received 13 September 2009; revised 29 November 2009; accepted 21 January 2010

length of polypeptide chain and the number of disulphide bonds, disintegrins are currently divided into five different groups including short-, medium-, long-chain disintegrins, dimeric disintegrins and disintegrins degraded from the C-termini of protein class III (P-III) snake venom metalloproteinases (SVMPs) (Gutierrez and Rucavado, 2000; Ramos and Selistre-de-Araujo, 2006). Based on the multi-domain organization, SVMPs are classified into four major protein groups: P-I (only a metalloproteinase domain), P-II (an additional disintegrin domain carboxy to the metalloproteinase domain), P-III (a disintegrin-like domain and a cysteine-rich domain carboxy to the metalloproteinase domain) and P-IV (a similar domain structure to the P-III SVMP, but with an additional lectin-binding domain). Most reported monomeric disintegrins have an Arg-Gly-Asp (RGD) or RGD-like tripeptide located at the tip of a loop formed by disulphide bonds that is responsible for their interactions with various integrins (Ramos and Selistre-de-Araujo, 2006). Metalloproteinase/disintegrin-like/cysteine-rich (MDC) domains-containing proteins are disintegrin analogues and act as integrin ligands. The integrin-binding motif in MDC proteins is X-Cys-Asp instead of the typical RGD. Another structure-relevant protein group found in mammals and other organisms is the family of disintegrin and metalloproteinase (ADAM) proteins (Gutierrez and Rucavado, 2000). The ADAM proteins are involved in several physiological processes and have a similar domain organization with extra transmembrane domain and intracellular domain. Both SVMPs and ADAMs belong to the Reprolysin family of metalloproteinases.

Numerous studies have demonstrated that SVMPs have multiple activities in the pathogenesis of local tissue damage such as releasing inflammatory mediators, degrading ECM components, as well as inducing haemorrhage (Gutierrez and Rucavado, 2000). Some of them also can inhibit platelet aggregation and degrade blood clotting factors. Recently, evidence has indicated that endothelial cells exposed to SVMPs may undergo apoptosis consequent on detachment from their substrate, usually the ECM, also known as anoikis, derived from the Greek word for homelessness (You *et al*., 2003; Diaz *et al*., 2005; Laing and Moura-da-Silva, 2005; Tanjoni *et al*., 2005). It is now well known that anoikis plays a pivotal role on tissue homeostasis *in vivo* and pathogenesis of vascular disease (Michel, 2003). Therefore, a useful strategy for treating anoikis-resistant cells with SVMP-derived agents in combination with conventional drugs will open a new avenue to restoration of tissue homeostasis and treatment of malignant diseases such as cancer.

A Glu-Cys-Asp (ECD)-containing proteinase, acurhagin (GenBank accession number AY566610), has been isolated from Formosan *Agkistrodon acutus* (*A. acutus*) venom and found to function as a P-III SVMP, based on its three-domain organization and enzymatic properties (Wang and Huang, 2002; Wang *et al*., 2005). In the present study, the biological activities of the C-terminal fragment of acurhagin, termed acurhagin-C, were further characterized using human umbilical vein endothelial cells (HUVECs). These data indicated that acurhagin-C inhibited endothelial cell adhesion and spreading on ECMs, followed by damage to cell functions and finally eliciting anoikis. The structural features and possible molecular mechanisms involved in these interactions of acurhagin-C and HUVEC were also investigated. On this evidence, acurhagin-C would be a potential anti-angiogenesis agent.

Methods

Purification of venom proteins

Acurhagin was purified from *A. acutus* venom according to the method described previously (Wang and Huang, 2002). Previously, it has been shown that the larger SVMPs may undergo autoproteolytic degradation. Acurhagin-C was thus obtained by incubating acurhagin with double distilled H_2O for several weeks at 4°C and then further purified through a gel-filtration column. The molecular weight of acurhagin-C, as determined by MALD-TOF mass spectrometry was 23.5 kDa, which is consistent with that of catrocollastatin-C, a C-terminal fragment from catrocollastatin (Shimokawa *et al*., 1997). Two other RGD disintegrins, arietin and triflavin, were purified from the venoms of *Bitis arietans* and *Trimeresurus flavoviridis* respectively (Wang *et al*., 2005). The protein purity was assessed by SDS-polyacrylamide gel electrophoresis (SDS-PAGE). Pooled pure fractions of these proteins were further tested for their functions.

Peptide synthesis

Two synthetic peptides RIARGDFPDDR (1316.6 Da) and RASMSECDPAEH (1332.2 Da), corresponding to RGD loop in triflavin and ECD loop in acurhagin-C, were purchased from GenScript (Piscataway, NJ, USA). The structure of both peptides were confirmed by mass spectrometry analysis and the peptides purified by reverse-phase high-performance liquid chromatography. The peptides with purity greater than 95% were used in functional assays.

Cell cultures

Human umbilical vein endothelial cells were thawed and grown to 80–90% confluence in medium 199 (M199) containing 10% fetal bovine serum (FBS), 5% (v/v) endothelial growth medium-2 (Clonetics, Walkersville, MD, USA) and 30 $\mu g \cdot mL^{-1}$ endothelial cell growth supplement (Upstate, Temecula, CA, USA). Cells were cultured at 37°C in the presence 5% CO_2 and serially passed in cell culture flasks (Wang, 2008). Confluent cultures between the third and sixth passages were washed with phosphate-buffered saline (PBS), harvested with 0.025% trypsin and 0.01% EDTA and counted with a haemocytometer before functional assays.

Cell viability assay

The viability assay was performed according to the manufacturer's instructions (Promega, Madison, WI, USA). After starvation, cells were harvested and treated with the indicated agents for 15 min at room temperature. The treated cells were subsequently seeded onto 96-well plate for 44 h. Following wash with PBS, cells were incubated with 3-[4, 5-dimethylthiazol-2-yl]-2, 5-diphenyl tetrazolium bromide (MTT) for 4 h. Formazan crystals resulting from MTT reduction were dissolved by adding stop solution and gently

agitated for 30 min. The absorbance of the supernatant was then measured spectrophotometrically at 560 nm.

Cell apoptosis assay

To quantify the sub-G1 population in cell cycle as a measurement of apoptosis, HUVECs in the absence or presence of various venom proteins were collected by centrifugation and adjusted to 2×10^6 cells·mL^{-1}. Prechilled ethanol was added into cell suspension for fixation and then incubated at 4°C overnight. After removing the ethanol, the DNAs of the cells were stained and analysed by flow cytometry.

Cell adhesion assay

Ninety-six-well microplates were pre-coated with various ECMs and left at 4°C overnight. The plates were then rinsed twice with PBS and blocked with 1% BSA for 1 h. Subsequently, HUVECs were incubated without or with acurhagin-C for 15 min on ice before being applied to the plates. Following incubation for 2 h in the plates, unattached cells were gently washed away with PBS. The attached cells were then fixed with 1% formaldehyde for 30 min at room temperature and stained with methylene blue (Oliver *et al*., 1989). The stained adherent cells were then photographed before lysis. The relative number of adherent cells was calculated by dissolving the stained cells with 50% ethanol and 50% hydrochloric acid and then reading the absorbance at 630 nm. The amount of non-specific adhesion was determined using wells pre-coated with BSA only.

Cell migration (haptotaxis) assay

Human umbilical vein endothelial cell migration assay was performed using 24-well companion plates and Transwell inserts sealed at one end with an 8 μm pore size PET membrane as described by manufacturer (BD Biosciences). The underside of the PET membrane was coated with vitronectin, or BSA, and the lower chamber was filled with M199. After treating HUVEC with venom protein, an aliquot of cell suspension was plated onto the upper chamber of Transwell. Following 24 h incubation, all non-migratory cells were removed from the upper surface of the membrane by scrubbing with a cotton swab, and the migrated cells were then fixed and stained with 4% paraformaldehyde and Wright-Giemsa respectively. Prior to the addition of extraction buffer, migrated cells were photographed by an inverted microscope (Nikon, Tokyo, Japan). The relative number of migratory cells was calculated by lysing the stained cells with 10% acetic acid and then reading the absorbance at 560 nm.

Cell invasion assay

The upper side of the filter membrane was firstly coated with Matrigel (BD Biosciences). Matrigel was diluted to 4 mg·mL^{-1} using serum-free M199 at 4°C, and an aliquot of Matrigel was added to each filter insert and incubated at 37°C for 30 min to form a uniform three-dimensional gel. The invasion assay was initiated by inoculating the upper chamber with cells that were either untreated or treated with venom protein and the lower chamber was filled without or with fibroblast growth factor (FGF)-2 as a chemoattractant. After treatment, the cells were incubated in a humidified incubator for 24 h. The cells that had invaded the Matrigel and moved to the lower surface of the filter membrane were fixed in 70% methanol and stained with Wright-Giemsa for 3 min. The upper surfaces of the filters were scraped with moist cotton swab to remove all non-invading cells and Matrigel. The chambers were washed three times with PBS and the invaded cells were then photographed and quantified as described for the cell migration assay.

Tube formation assay on Matrigel

Matrigel tube formation assays were performed as described previously with minor modification (Mousa and Mohamed, 2004). Matrigel was diluted to 4 mg·mL^{-1} in the presence of FGF2 and added to the base of the well in a 24-well plate to form a gel layer. After incubation without or with tested samples for 18 h, HUVECs were stained with Wright-Giemsa and photographed under microscope.

Chick chorioallantoic membrane (CAM) assay

Fertilized eggs of 10-day-old chick embryos were opened with a window (1.0 cm^2) that allowed direct access to the underlying CAM as described previously (Colman *et al*., 2000). Filter paper discs (1.3 cm, Minipore, Billerica, MA, USA) were soaked in cortisone (3 mg·mL^{-1})/ethanol (95%) and subsequently air-dried under sterile conditions. The sterile paper discs were then saturated with test samples in a total volume of 20 μL and applied to the top of the CAM. The window was covered with sterile cellophane tape, and the embryos were incubated for 48 h (37°C/60% humidity) to develop spontaneous angiogenesis. Tube length of each randomly chosen field was quantified using image analysis software of AngiogenesisImage Analyzer (Kurabo, Osaka, Japan).

Cell proliferation assay

Human umbilical vein endothelial cells were firstly allowed to grow onto 96-well plate pre-coated with various ECMs for 2 h at 37°C. Subsequently, an aliquot of FGF2-containing medium without or with various tested agent was added to each well, followed by 12 h incubation. The number of living cells was then measured by adding MTT as described above. Absorbance at 560 nm of individual wells was measured to determine the relative cell number.

Flow cytometry

For detecting the cell surface target for binding acurhagin-C on cell surface, HUVECs were fixed with 1% paraformaldehyde for 30 min at 4°C. After washing with PBS, cells were incubated with fluorescein isothiocyanate (FITC)-conjugated antibody for 30 min on ice with gentle shaking. After incubation with FITC probe, cells were analysed with FACS Calibur and CellQuest software (BD Biosciences) using excitation and emission wavelengths of 488 and 525 nm respectively. Fluorescence signals from gated cells were collected to

calculate fluorescence intensity of single cell. To examine the interaction site on HUVEC membranes, acurhagin-C was pre-incubated with HUVEC for 30 min on ice prior to the addition of primary antibody.

Binding of purified αvβ3 to immobilized venom proteins
Venom proteins and BSA were, respectively, diluted with PBS and immobilized on a 96-well ELISA plate for 12 h at 4°C. After blocking the wells with 1% BSA in PBS containing 0.02% Tween (PBS-T), purified αvβ3 (1 μg per well) was then added to the wells and the plate was incubated for 30 min at 37°C. Binding of the anti-αvβ3 mAb LM609 to the bound receptor was assessed using a horseradish peroxidase (HRP)-goat anti-mouse IgG according to the Protein Detector HRP ELISA kits (KPL; Gaithersburg, MD, USA).

Apoptotic DNA fragmentation assay
DNA extraction from apoptotic cells for DNA fragmentation analysis was performed according to the manufacturer's instructions (Promega, Madison, WI, USA). Briefly, pretreated HUVECs were washed, lysed and fixed with PBS, lysis buffer and 70% ethanol respectively. After DNA extraction, the mixture was analysed on 1% agarose gel. DNA ladders stained by ethidium bromide were visualized under UV light.

Immunoblotting
Cell lysates from HUVECs were electrophoresed on SDS-PAGE and transferred to polyvinyldifluoride membrane. The blocked membranes were then incubated with the indicated antibody, and the immunoreactive bands were visualized using chemiluminescent reagent as recommended by manufacturer (Pierce, Rockford, IL, USA).

Statistical analysis
Data were expressed as mean ± SEM. Student's *t*-tests were used to assess the significance of differences between means.

Materials
Human umbilical vein endothelial cells were purchased from Cascade Biologics (Portland, OR, USA). Lyophilized snake venoms of *A. acutus* (Taiwan), *B. arietans* and *T. flavoviridis* were from Latoxan (Rosans, France). Human fibronectin, vitronectin, FGF2, staurosporine and extracellular signal-regulated kinase (ERK) inhibitor PD98059 were from Sigma Chemical (St Louis, MO, USA). Pan-caspase inhibitor (Z-VAD-FMK), caspase-1 inhibitor (Z-WEHD-FMK), caspase-3 inhibitor (Z-DEVD-FMK), negative caspase inhibitor (Z-FA-FMK) and caspase-3 substrate (Ac-DEVD-pNA) were from Promega (Madison, WI, USA). Matrigel and anti-glycoprotein (GP)Ibα monoclonal antibody (mAb) SZ2 (Andrews and Berndt, 1998) were from BD Biosciences (Bedford, MA, USA) and Beckman Coulter (Marseille, France) respectively. Anti-GPIbα mAb AP1 (Andrews and Berndt, 1998) and anti-αvβ3/αIIbβ3 mAb 7E3 (Yeh *et al*., 2000) were kindly donated by Drs R Montgomery and BS Coller respectively. Anti-αvβ3 mAb LM609 (Frangie *et al*., 2006) and purified αvβ3 were from Chemicon (Temecula, CA, USA). Anti-integrin α2 mAb FITC-AK7 (Kamiguti *et al*., 1996) was from BioLegend (San Diego, CA, USA). Anti-αvβ3 mAb FITC-23C6 (Takahashi *et al*., 1999), anti-focal adhesion kinase (FAK) mAb H-1 (Boutahar *et al*., 2004), anti-phosphorylated phosphatidylinositol 3-kinase (PI3K) p85α (Tyr508) polyclonal antibody (pAb), anti-PI3K p85α mAb B-9, anti-phosphorylated Akt (Ser473) pAb, anti-Akt mAb B-1, anti-caspase-3 mAb E-8, anti-poly(ADP-ribose) polymerase (PARP) mAb F-2 and HRP-goat anti-mouse IgG were from Santa Cruz Biotechnology (Santa Cruz, CA, USA). An anti-phosphorylated FAK (Tyr397) pAb was from BioSource (Camarillo, CA, USA).

Results

Effects of acurhagin-C on HUVEC viability and apoptosis
Acurhagin, a versatile 48 kDa SVMP, contains the typical three domains, an N-terminal 24.5 kDa metalloproteinase domain and followed by C-terminal 23.5 kDa disintegrin-like/cysteine-rich domains. Typically, acurhagin with 421-amino-acid residues has a Zn^{2+}-binding motif, $HEMGHNLGIHHD^{145–156}$, in the metalloproteinase domain and an essential recognition sequence, $ECD^{277–279}$, in the disintegrin-like domain (Figure 1A; Wang *et al*., 2005). In anchorage-dependent HUVECs, preliminary experiments showed that acurhagin may decrease the adhesion of suspended cells, but could not induce detachment of adherent cells. Thereafter, the studies of acurhagin on HUVEC functions were further investigated. HUVEC viability after serum deprivation was unaffected by 1 μM BSA compared with PBS, but 0.2 μM acurhagin and 0.4 μM acurhagin-C decreased viability by about 50% (Figure 1B). The RGD disintegrin, 0.5 μM triflavin also decreased endothelial viability by 20% but the medium-chain disintegrin arietin, even at 1 μM, did not change viability. These findings suggested that acurhagin-C was more potent than disintegrins in reducing HUVEC viability. To clarify whether the decreased endothelial cell viability after acurhagin was similar to the effect of a P-III SVMP jararhagin, which induces a specialized form of apoptosis (Tanjoni *et al*., 2005), flow cytometric analysis was subsequently performed to examine DNA content. Figure 1Ca shows a normal cell cycle stage including G0/G1, S and G2/M phases in PBS-treated HUVEC, and the sub-G1 phase represents cell undergoing apoptosis-associated DNA degradation under experimental conditions (4.18%). By contrast to a potent apoptosis inducer, staurosporine ($0.5\ \mu g \cdot mL^{-1}$), acurhagin (0.2 μM) also significantly induced HUVEC apoptosis (Figure 1Cb,c). However, acurhagin-C showed a dose-dependent increase of HUVEC apoptosis over the concentration range used (0.2–0.8 μM) (Figure 1Cd–f).

Effect of acurhagin-C on HUVEC adhesion to various immobilized ECMs
Recently, Tanjoni *et al*. (2005) proposed that the endothelial apoptosis induced by jararhagin followed the loss of adhesion by endothelial cells. To investigate if acurhagin-C induced apoptosis in HUVECs by the same mechanism as jararhagin,

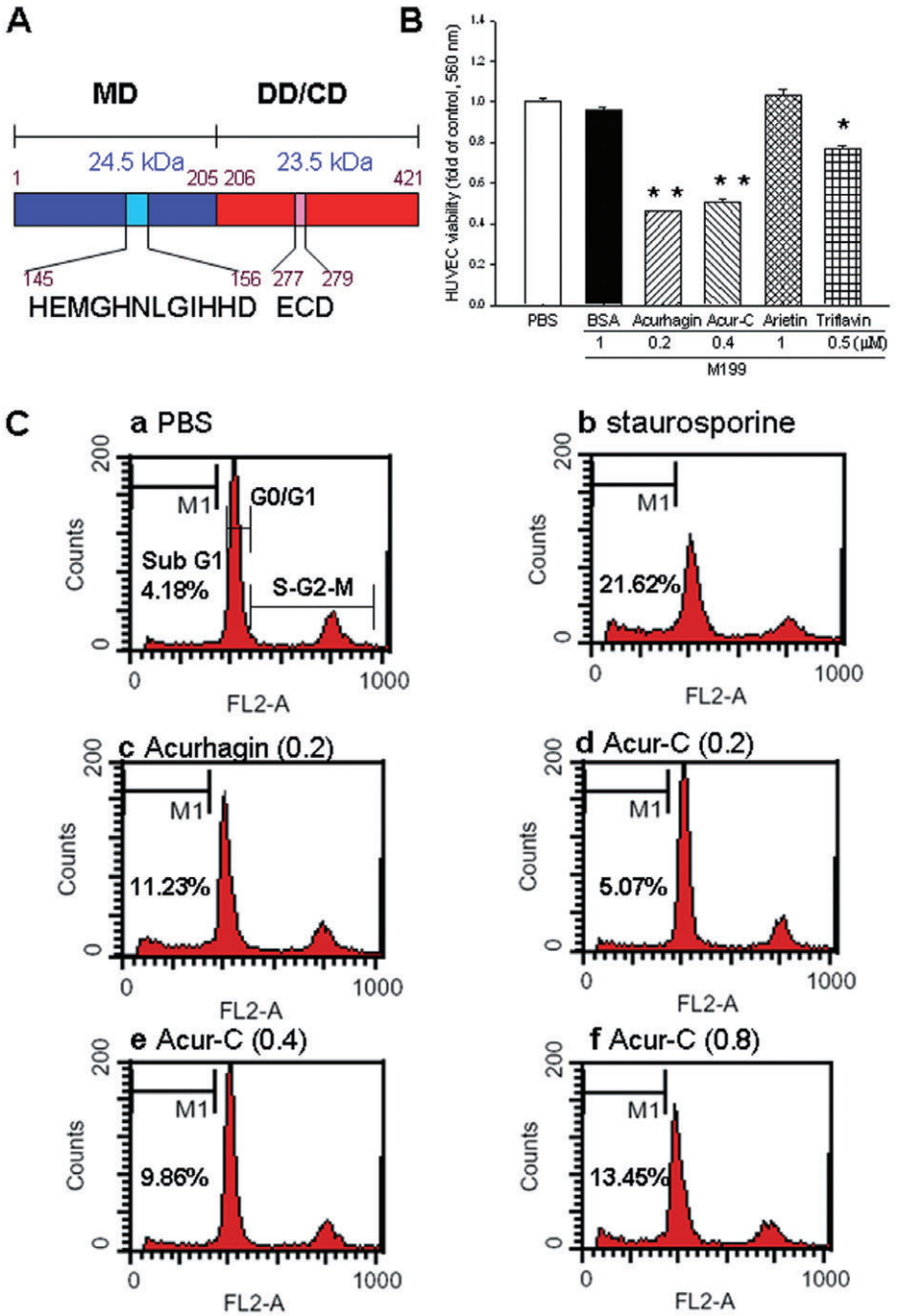

Figure 1 Effects of acurhagin-C on HUVEC viability and apoptosis. (A) Schematic structure of acurhagin. The apparent molecular weights of N-terminal metalloproteinase domain (MD) and C-terminal disintegrin-like/cysteine-rich domains (DD/CD) in the acurhagin molecule are shown as indicated. (B) After pretreatment with PBS, BSA, acurhagin, acurhagin-C (Acur-C), arietin or triflavin, HUVECs (1×10^4 cells per well) in serum-free M199 were seeded onto 96-well plates at 37°C/5% CO_2 for 44 h and followed by MTT assay. The absorbance was measured at 560 nm. All experiments were performed in quadruplicate and similar results were repeated at least three times. Results are expressed as relative activity on HUVEC viability (fold of control) and presented as mean ± SEM ($n = 4$). *$P < 0.05$; **$P < 0.01$ as compared with control. (C) HUVECs cultured in 10% FBS/M199 were treated with PBS (a), staurosporine (b, 0.5 μg·mL^{-1}), acurhagin (c, 0.2 μM) or acurhagin-C (d–f; 0.2, 0.4 and 0.8 μM) for 20 h and then fixed with 70% ethanol, permeabilized with 0.5% Triton X-100 containing 0.05% RNase, stained with propidium iodide and analysed by flow cytometry. The sub-G1 region represents cells undergoing apoptosis-associated DNA degradation and is expressed as a percentage with respect to the entire cell cycle. ECD, Glu-Cys-Asp; FBS, fetal bovine serum; HUVEC, human umbilical vein endothelial cell; MTT, 3-[4, 5-dimethylthiazol-2-yl]-2, 5-diphenyl tetrazolium bromide; PBS, phosphate-buffered saline.

cell adhesion assays were performed. As shown in Figure 2A, acurhagin-C inhibited HUVEC adhesion to immobilized fibronectin, collagen I and vitronectin in a concentration-dependent manner with IC_{50} values of approximately 0.6, 0.3 and 0.1 μM respectively. Morphological analysis showed that HUVEC adhering to ECMs in the absence of acurhagin-C, showed extensive spreading and formed spindle shapes. Although there was some spreading of acurhagin-C-treated

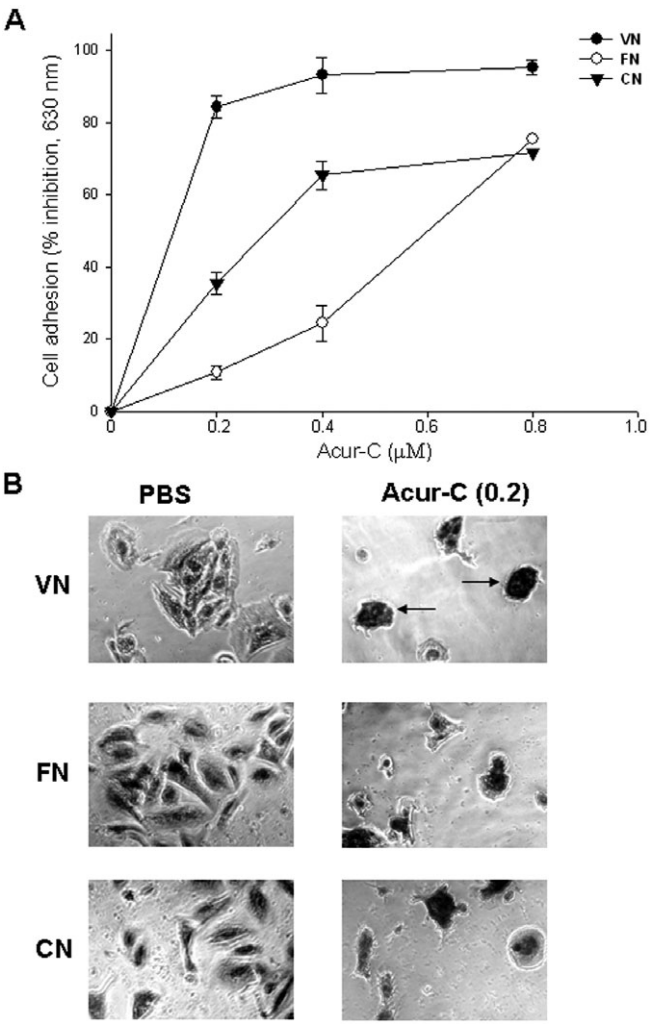

Figure 2 Acurhagin-C inhibited adhesion of human umbilical vein endothelial cells (HUVECs) to immobilized extracellular matrix (ECM) components. (A) HUVECs (2×10^4 cells per well) were seeded onto 96-well plates, which were pre-coated with various ECM components (1 μg per well; fibronectin, FN; collagen I, CN; vitronectin, VN), in the absence [phosphate-buffered saline (PBS) added] or presence of the indicated concentrations of acurhagin-C. After 2 h incubation at 37°C/5% CO_2, the attached cells were fixed and stained with 1% methylene blue/0.01 M borate, pH 8.5. The cells were then lysed and an optical density reading at 630 nm was taken. All experiments were conducted in quadruplicate and repeated at least three times. For a negative control, BSA (1%)-coated wells were used, and these values have been subtracted from those from assays with FN, CN or VN. Data are presented as mean ± SEM ($n = 4$). Note that acurhagin-C at 0.2 μM showed most potent inhibition on HUVEC adhesion to vitronectin. (B) Morphology of HUVEC adhering to fibronectin, collagen I and vitronectin in the absence or presence of acurhagin-C (Acur-C; 0.2 μM). After washing and fixation, pretreated cells were photographed under a phase-contrast microscope at 100× original magnification. The arrows show acurhagin-C-treated HUVEC adhering to immobilized vitronectin without spreading (rounded up cells).

HUVEC on fibronectin- or collagen I-coated wells, the shape of cells adhering onto vitronectin-coated wells remained rounded and they did not spread (Figure 2B).

Effects of acurhagin-C on HUVEC migration and invasion

The induction of migration by ECMs can be defined as haptotaxis when substratum-bound and chemotaxis when the ligand is soluble (Aznavooriant *et al*., 1996). To explore the effects of acurhagin-C on the haptotactic migration of HUVECs towards immobilized proteins, the assay chambers pre-coated with vitronectin, or BSA (as a control), and cell migration was observed by a phase-contrast microscope. As shown in Figure 3Aa–c, HUVECs significantly migrated to the underside of filter membranes coated with vitronectin, but not those coated with BSA, and triflavin strongly inhibited such migration. Figure 3Ad–f indicates that acurhagin-C dose-dependently blocked HUVEC migration towards the vitronectin-coated membrane. These migration assays were quantified by a colorimetric method and the results showed that the inhibition of HUVEC migration towards vitronectin by acurhagin-C was concentration-dependent with an IC_{50} value of about 0.2 μM (Figure 3C).

In order to assess the effects of acurhagin-C on invasion by HUVEC, Matrigel invasion chambers were used. As shown in Figure 3Ba,b, FGF2 significantly promoted HUVEC invasion of the Matrigel. Such invasion was inhibited by triflavin and by increasing concentrations of acurhagin-C, yielding a IC_{50} of about 0.1 μM (Figure 3Bb,d–f,C).

Inhibition of FGF2-induced angiogenesis both in vitro *and* in vivo *by acurhagin-C*

Angiogenesis, a complex process, is modulated overall by the specific interactions of endothelial cells with a variety of adhesion molecules and cytokines. Generally, the integrins αvβ3 and αvβ5 are required for FGF2- and VEGF-primed angiogenesis respectively (Friedlander *et al*., 1995). To examine the effect of acurhagin-C on HUVEC differentiation into vascular structures, a Matrigel-based tube formation assay was conducted and HUVECs treated with various reagents were grown on FGF2-containing Matrigel, followed by microscopic observation. As shown in Figure 4Aa, PBS-treated cells displayed high motility and aligned into a network-like structure after seeding on Matrigel. Although triflavin and acurhagin-C, at the same concentration of 0.4 μM, significantly suppressed FGF2-stimulated formation of tube-like structures, acurhagin at 0.2 μM completely prevented FGF2-induced angiogenesis, leading to the formation of multicellular aggregates in the Matrigel (Figure 4Ab–d). To assess the contribution of angiogenesis mediated through the integrin and/or non-integrin adhesion molecules, such as the GPIb complex (Tan *et al*., 1999; Yeh *et al*., 2000), antibodies against αvβ3 and GPIbα were used. As expected, anti-αvβ3 antibodies 7E3 and LM609 (Figure 4Ae,f) showed stronger inhibition of FGF2-induced tube formation than anti-GPIbα antibodies AP1 and SZ2 (Figure 4Ag,h), suggesting this model of angiogenesis *in vitro* was αvβ3-dependent.

To clarify whether acurhagin-C affected FGF2-stimulated angiogenesis *in vivo*, the CAM assay was used to assay neovascularization (Bischoff, 1995). Following 48 h incubation in the presence of FGF2, CAMs treated with PBS were well vascularized (Figure 4Ba), whereas those treated with an ERK inhibitor PD98059 and the anti-αvβ3 antibody LM609 showed clearly reduced blood vessel formation (Figure 4Bb,c). Quantitative assessment of tube length (Figure 4C) also showed that activation of ERK was involved in the angiogenesis stimulated by FGF2. Further, acurhagin-C

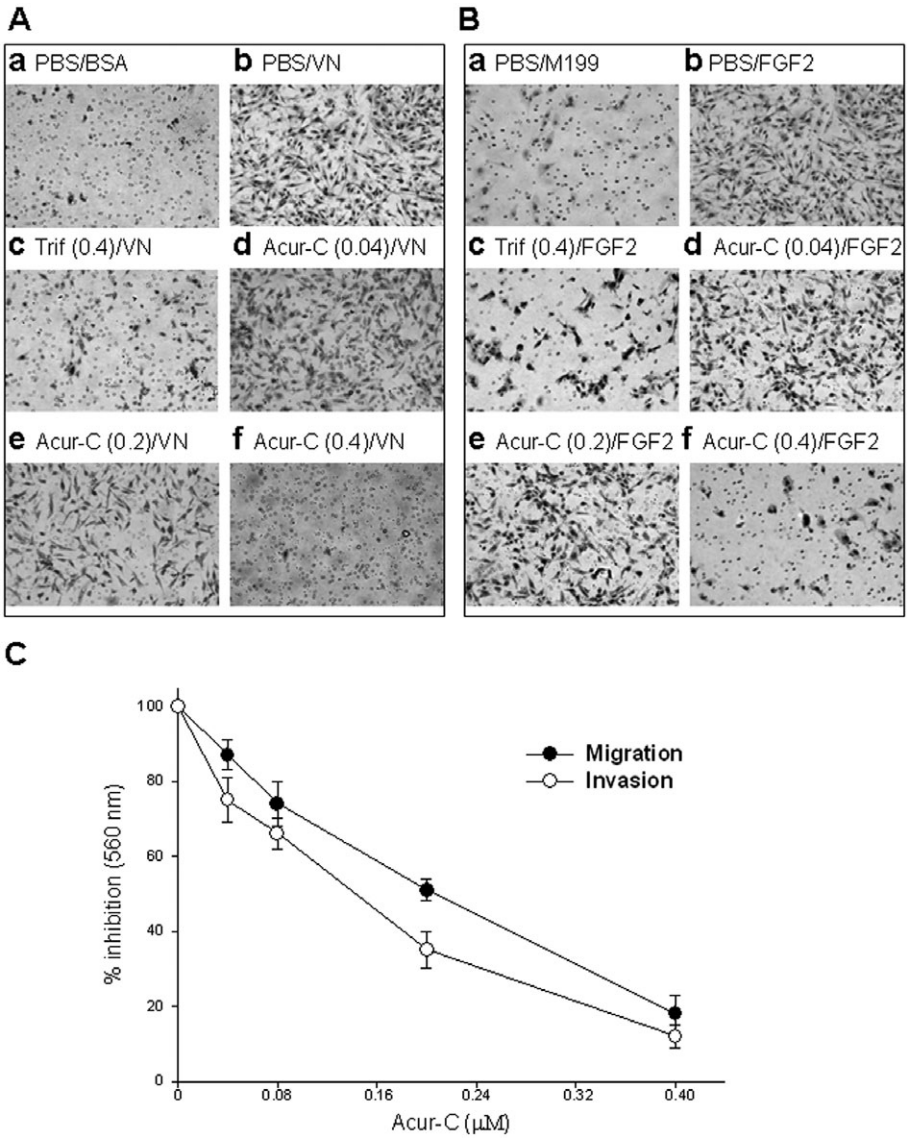

Figure 3 Effects of acurhagin-C on human umbilical vein endothelial cell (HUVEC) migration and invasion. (A) The lower surface of chamber filters were pre-coated with BSA (a, 2 μg per well), or vitronectin (VN, b–f, 2 μg per well), and the migration assay was performed. HUVECs (1×10^5 cells per well) were pre-incubated with phosphate-buffered saline (PBS) (a,b), triflavin (c, Trif, 0.4 μM) or acurhagin-C (Acur-C; d–f; 0.04, 0.2, 0.4 μM) for 30 min, respectively, and then plated onto the upper chamber of Transwells and allowed to migrate for 24 h. Following fixation and removal of non-migrated cells, cells that migrated to the underside of filter membrane were photographed by phase-contrast microscope (100× original magnification). (B) HUVECs (3×10^5 cells per well) were, respectively, incubated with various agents [a,b, PBS; c, triflavin (0.4 μM); d–f, acurhagin-C (Acur-C; 0.04, 0.2 and 0.4 μM)] in the upper insert chambers and then allowed to invade the Matrigel-coated filter membranes to the lower chambers in the absence (a, M199 added) or presence of fibroblast growth factor-2 (FGF2) (b–f, 20 ng·mL^{-1}) for 24 h. After fixation and removal of non-invasive cells, cells invading to the underside of filter membrane were photographed. (C) The inhibition of acurhagin-C on vitronectin-induced migration and FGF2-induced invasion were quantified by ELISA assay (560 nm). The indicated concentrations of acurhagin-C were used for determining the IC_{50} values. All experiments were performed in quadruplicate, and similar results were obtained at least three times. Data are presented as mean ± SEM ($n = 4$).

dose-dependently disrupted spontaneous angiogenesis but did not affect existing vessels in the same CAMs. These findings confirmed that acurhagin-C was a potent inhibitor of FGF2-primed angiogenesis *in vivo*.

Interactions of acurhagin-C with endothelial integrin αvβ3

In order to assess the contribution of specific interactions of acurhagin-C with endothelial integrin αvβ3, to the inhibition of angiogenesis, binding studies were performed to determine the binding sites of acurhagin-C. On HUVECs, the integrins αvβ3 and α2β1 are reported to be critical to adhesion to vitronectin and collagen respectively. To prevent receptor internalization leading to decreased immunoreactivity, a preparation of formalin-fixed HUVEC suspension was used in flow cytometric analysis. As shown in Figure 5Aa,b, the coexistence of integrins αvβ3 and α2β1 on HUVEC could be, respectively, detected by FITC-23C6 (against αvβ3) and FITC-AK7 (against α2). However, only the immunoreactivity of 23C6 was reduced after pretreatment with acurhagin-C,

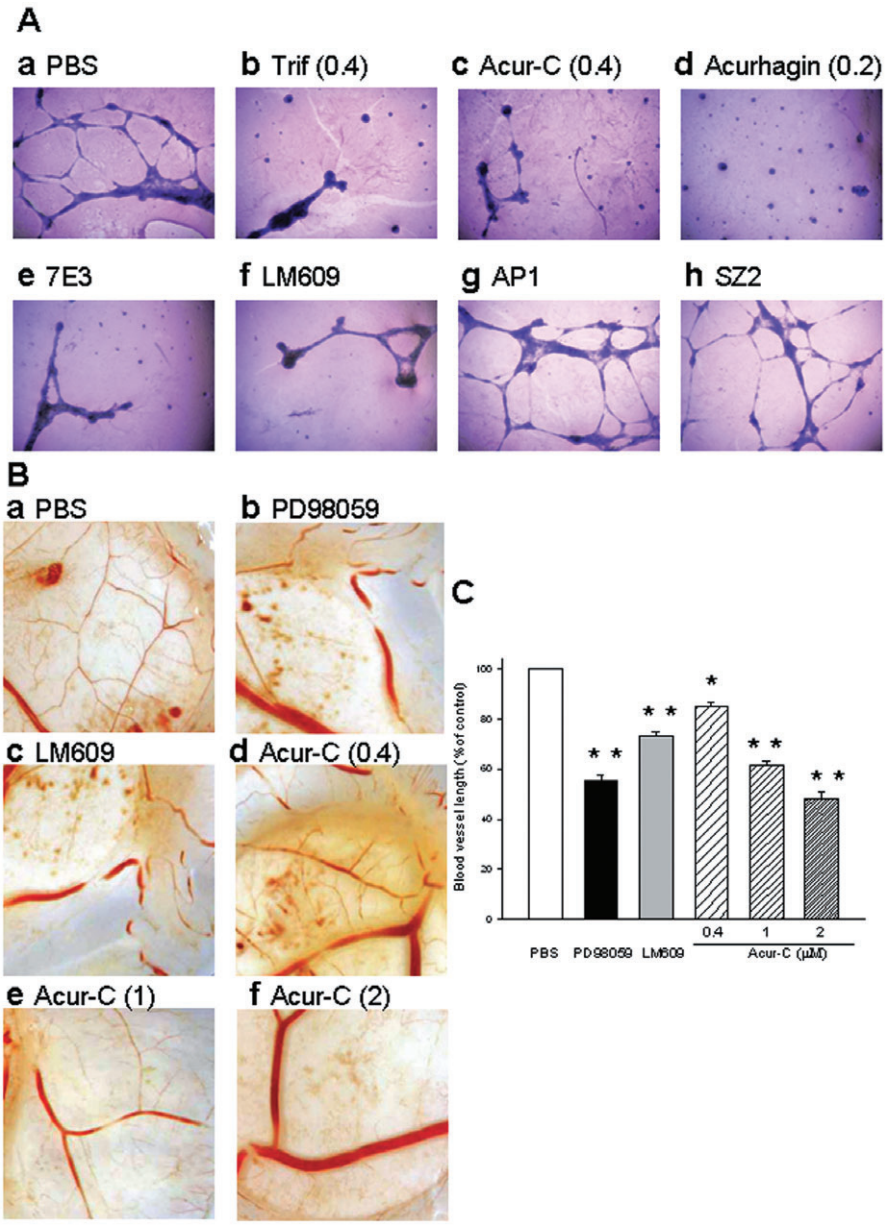

Figure 4 Effects of acurhagin-C on fibroblast growth factor-2 (FGF2)-induced angiogenesis *in vitro* and *in vivo*. (A) HUVECs (1×10^5 cells per well) were pre-incubated with phosphate-buffered saline (PBS) (a), triflavin (b, Trif; 0.4 μM), acurhagin-C (c, Acur-C; 0.4 μM), acurhagin (d, 0.2 μM), the antibodies 7E3 (e, 20 μg·mL^{-1}), LM609 (f, 20 μg·mL^{-1}), AP1 (g, 20 μg·mL^{-1}) or SZ2 (h, 20 μg·mL^{-1}) in the presence of FGF2 (20 ng·mL^{-1}), respectively, for 15 min at room temperature and then plated on Matrigel-coated wells for 18 h at 37°C. After washing and fixation, cells were photographed under a phase-contrast microscope at 40× original magnification. (B) Chick chorioallantoic membrane (CAM) assay. Filter discs soaked in FGF2 (20 ng per egg) in the absence (a, PBS-treated) or presence of PD98059 (b, 20 μM), LM609 (c, 50 μg·mL^{-1}) or acurhagin-C (d–f, 0.4, 1, 2 μM) were applied on 10-day-old CAMs. After 48 h incubation, CAMs were removed, fixed and photographed. This is representative of eight similar experiments. (C) The level of angiogenesis in FGF2-treated CAMs in the absence or presence of PD98059, LM609 or acurhagin-C (Acur-C) was quantified by counting blood vessel length. Results are expressed as % of control and presented as mean ± SEM ($n = 8$). *$P < 0.05$; **$P < 0.01$ as compared with control.

implying competition between acurhagin-C and 23C6 for binding to HUVEC. Thus, these findings indicated that only αvβ3 was involved in the interactions of acurhagin-C with HUVEC and the binding epitope of acurhagin-C on αvβ3 may be identical or overlap with that recognized by the antibody 23C6.

In terms of the primary protein sequences, the sequence of CRIARGDFPDDRC in triflavin is positionally analogous to that of CRASMSECDPAEHC in acurhagin-C (Wang *et al.*, 2005). Based on these structures and after deleting the N- and C-terminal cysteines, as the original linkage of disulfide bond in acurhagin-C is difficult to determine, two linear peptides termed RGD peptide (11 amino acids) and ECD peptide (12 amino acids) were designed and synthesized. As shown in Figure 5B, triflavin (0.5 μM) and acurhagin-C (0.4 μM) exhibited potent inhibition of the binding of FITC-23C6 to

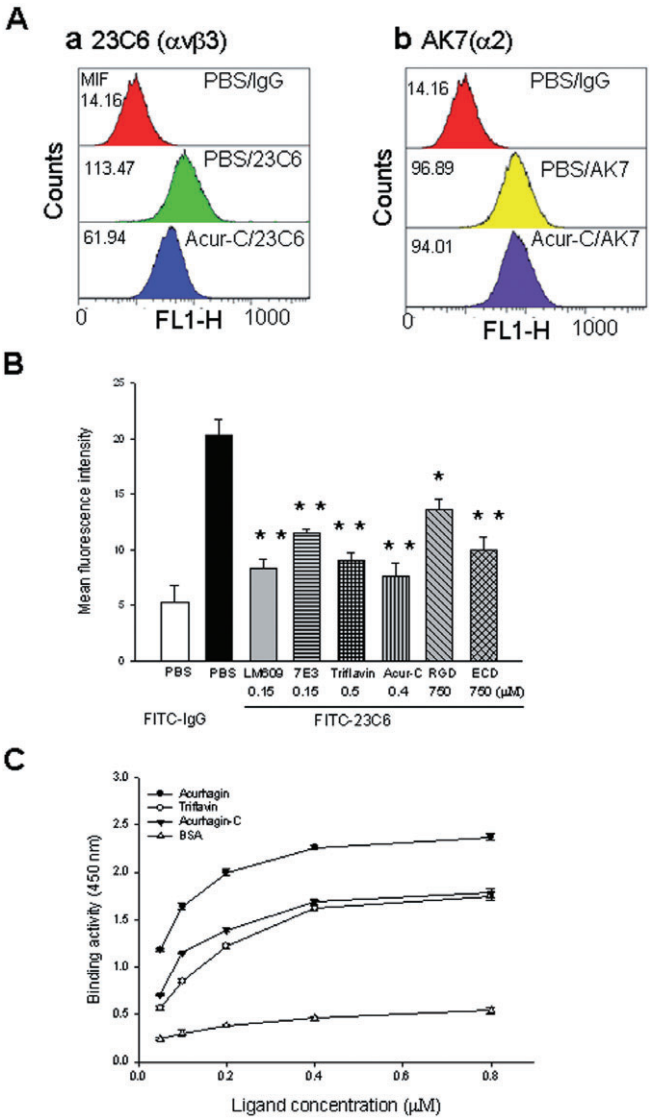

Figure 5 Interaction of acurhagin-C with integrins on human umbilical vein endothelial cells (HUVECs). (A) Following the incubation of HUVECs (1×10^6 cells·mL^{-1}) without [phosphate-buffered saline (PBS) added; the middle panel] or with acurhagin-C (Acur-C; 0.4 μM, the lower panel) for 30 min on ice, fluorescein isothiocyanate (FITC)-conjugated antibody (a, 23C6; b, AK7; 10 μg·mL^{-1}) or non-immune FITC-IgG (as a negative control; 1:50 dilution, the upper panel) was subsequently added to HUVECs for additional 30 min incubation and then analysed by flow cytometry. Histograms show the fluorescence intensity of mAbs bound to PBS- or acurhagin-C-treated HUVECs. Results are shown in mean fluorescence intensity (MFI) and one of three similar experiments is presented. (B) Quantitative analyses for the binding of FITC-23C6 in the absence or presence of mAbs (LM609; 7E3), venom proteins (triflavin; acurhagin-C), or synthetic peptides [Arg-Gly-Asp (RGD) peptide, RGD; Glu-Cys-Asp (ECD) peptide, ECD]. Results are presented as MFI ± SEM ($n = 4$). *$P < 0.05$; **$P < 0.01$ as compared with control. (C) A 96-well plate was pre-coated with various concentrations of acurhagin, triflavin, acurhagin-C or BSA. After blocking with 1% BSA in PBS-T for 1 h, purified αvβ3 (1 μg) was then added to each well and the plate was incubated for an additional 30 min at 37°C/5% CO_2. After extensive washing with PBS-T, the anti-αvβ3 mAb LM609 was used as primary antibody. After 1 h incubation at 37°C and subsequent washing, horseradish peroxidase-IgG was used as the secondary antibody. Absorbance at 450 nm of the individual well was measured to determine the relative binding activity.

HUVEC, which is consistent with the effects of the anti-αvβ3 antibodies LM609 and 7E3. As expected, both synthetic peptides, at a higher concentration 750 μM, also had the same inhibitory effects as their parent molecules.

Binding of purified αvβ3 to immobilized acurhagin-C

As αvβ3 is the most abundant receptor on HUVEC, the interaction of purified αvβ3 with immobilized acurhagin-C was analysed by ELISA assay. As shown in Figure 5C, the purified αvβ3 bound to immobilized acurhagin-C in a concentration-dependent manner. Notably, acurhagin-C showed a lesser binding capacity but a similar pattern to that with acurhagin, suggesting that the participation of the metalloproteinase domain could contribute to the interactions of acurhagin with αvβ3. Triflavin had the same binding capacity as acurhagin-C. Taken together, these data imply that the motifs RGD and ECD are both major recognition sequences. However, some unidentified motifs in the metalloproteinase domain of acurhagin remain to be characterized.

Acurhagin-C directly induces endothelial apoptosis via the activation of caspase-3

To elucidate the mechanism of endothelial apoptosis induced by acurhagin-C, DNA fragmentation was analysed by agarose gel electrophoresis. Following incubation in growth factor-free medium, the genomic DNA of adherent and suspended HUVECs was isolated for analysis. Relative to the effects of PBS (Figure 6A, lane 1), a pan-caspase inhibitor Z-VAD-FMK (25 and 50 μM) concentration-dependently suppressed acurhagin-C-induced DNA fragmentation in HUVEC after 20 h incubation (Figure 6A, lanes 2 and 3). Recently, Tabruyn *et al*. (2003) indicated that caspase-3 is involved in the apoptotic action of a 16 kDa fragment of human prolactin in bovine capillary endothelial cells. Thus, caspase-3 activation assay was performed in acurhagin-C-treated HUVEC and showed that caspase-3 activity significantly increased after treating HUVEC with acurhagin-C (Figure 6B). However, the pan-caspase inhibitor Z-VAD-FMK and a selective caspase-3 inhibitor Z-DEVD-FMK strongly inhibited the endothelial apoptosis triggered by acurhagin-C. By contrast, a caspase-1 inhibitor Z-WEHD-FMK and a negative caspase inhibitor Z-FA-FMK had no such effect, indicating the apoptotic process induced by acurhagin-C was caspase-3-dependent. The appearance of an 85 kDa fragment of PARP, produced by activated caspase-3, is considered a marker of the execution stage of apoptosis. As shown in Figure 6C, activation of procaspase-3 and the cleaved 85 kDa PARP fragment could be observed after 60 min treatment with acurhagin-C, suggesting that the apoptotic pathway was initiated about 1h after the exposure of HUVECs to acurhagin-C.

Molecular mechanisms of endothelial anoikis elicited by acurhagin-C

To examine how the biological activity of acurhagin-C was correlated with the processes of neovascularization, HUVEC proliferation assays, using ECM components and FGF2, were performed. As shown in Figure 7A, acurhagin-C inhibited

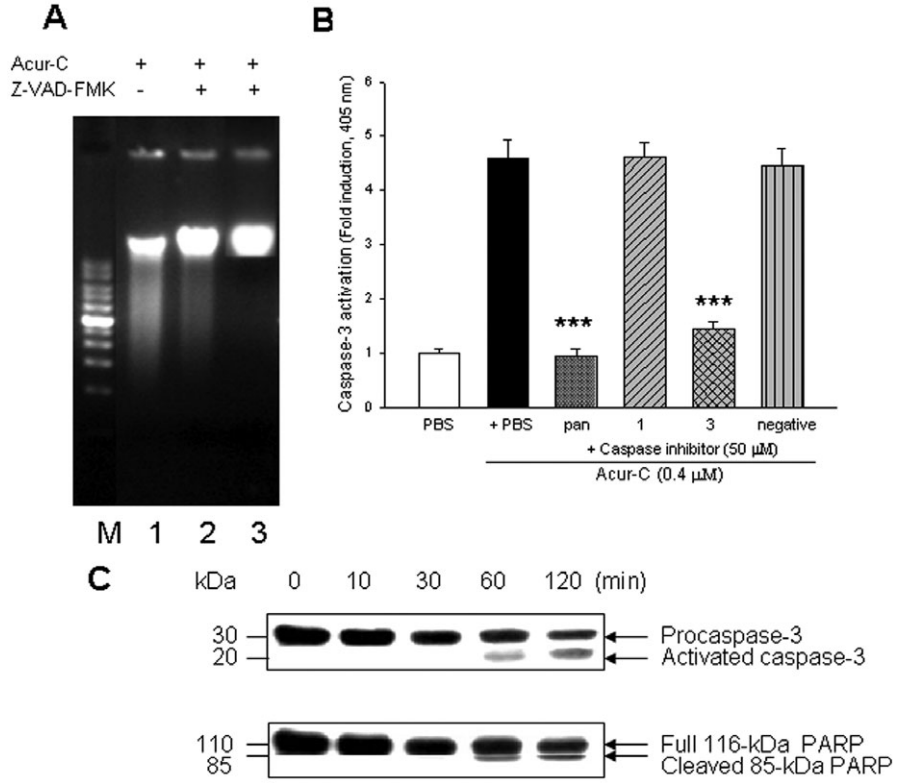

Figure 6 Analyses of DNA fragmentation, caspase-3 activation and poly(ADP-ribose) polymerase (PARP) cleavage in acurhagin-C-treated human umbilical vein endothelial cell (HUVEC). (A) The adherent and suspended cells were collected after incubation with acurhagin-C (0.4 μM) without (lane 1, DMSO) or with a pan-caspase inhibitor Z-VAD-FMK (lanes 2 and 3; 25, 50 μM) for 20 h and then lysed. Genomic DNA was isolated and subjected to electrophoretic separation on a 1% agarose gel. The internucleosomal DNA fragmentation is represented as oligonucleosomal banding at lower molecular weight. A 100 bp ladder is shown in lane M. This result is representative of three separate experiments. (B) Following the 16 h incubation at 37°C, untreated [phosphate-buffered saline (PBS) added] and acurhagin-C (Acur-C; 0.4 μM)-treated cells in the absence or presence of various caspase inhibitors as indicated (pan-caspase inhibitor, pan; caspase-1 inhibitor, 1; caspase-3 inhibitor, 3; negative caspase inhibitor, negative) were collected and then lysed for analysis. The cell extracts were reacted with chromogenic substrate DEVD-p-nitroaniline for 4 h at 37°C, and the absorbance at 405 nm was measured as caspase-3 activation (fold induction). Results are presented as mean ± SEM ($n = 4$). ***$P < 0.001$ as compared with control. (C) Cells were treated with acurhagin-C (0.4 μM) for the indicated time intervals at 37°C and then lysed with reducing sample buffer. Subsequently, cell lysate was subjected to 10% SDS-PAGE and electroblotted onto a polyvinyldifluoride membrane. The activation of procaspase-3 and cleavage of endogenous PARP by caspase-3 were detected using anti-caspase-3 and anti-PARP antibodies respectively.

HUVEC proliferation in vitronectin-coated wells, in the presence of FGF2 but had little effect in the absence of FGF2. The antibody LM609 and the ECD peptide also significantly and specifically reduced HUVEC proliferation on vitronectin, but not fibronectin (Figure 7B). From these results it seems that acurhagin-C specifically binds to integrin αvβ3, which is closely associated with FGF2-induced HUVEC proliferation. In addition, blocking αvβ3 by acurhagin-C may result in unscheduled apoptosis among proliferating vascular cells. Currently, the mechanism of angiogenesis can be divided generally into three phases: initiation, proliferation/invasion and differentiation (Stromblad and Cheresh, 1996). During the proliferative and invasive phases of angiogenesis, the integrin αvβ3 is preferentially expressed on vascular cells. The ECD-containing peptide also inhibited FGF2-induced HUVEC invasion (Figure 7C).

To explore the mechanism of acurhagin-C-induced endothelial apoptosis, the role of caspases in such anti-invasive effects was observed. The caspase-3 inhibitor Z-DEVD-FMK but not the caspase-1 inhibitor Z-WEHD-FMK blocked the inhibition by ECD peptide (750 μM) of FGF2-induced HUVEC invasion. We also assessed the role of caspase-3 in the angiogenesis model of tube-like structures formed by HUVECs in Matrigel after induction by FGF2. As shown in Figure 7D, both acurhagin-C (0.4 μM) and ECD peptide (750 μM) inhibited this *in vitro* model of angiogenesis. Once again, the caspase-3 inhibitor suppressed the inhibition by acurhagin-C, or by ECD peptide, in this model.

Previously, it has been well established that integrin activation may lead to the phosphorylation of FAK, a tyrosine kinase prominently localized at focal adhesions (Boudreau and Jones, 1999). Assays, using an anti-FAK antibody, indicated that acurhagin has little effect on the degradation of focal adhesions during 12 h incubation (data not shown). However, following the treatment of endothelial cells with acurhagin-C for 30 min and then stimulation of the acurhagin-C-treated cells with FGF2 for an additional 30 min, acurhagin-C was shown to decrease the level of phosphorylated FAK (Tyr397) in a concentration-dependent manner (Figure 7E, the upper panel). The phosphorylation of PI3K and Akt are two critical events downstream of the FAK in the cell survival pathway (Grossmann, 2002). As shown in

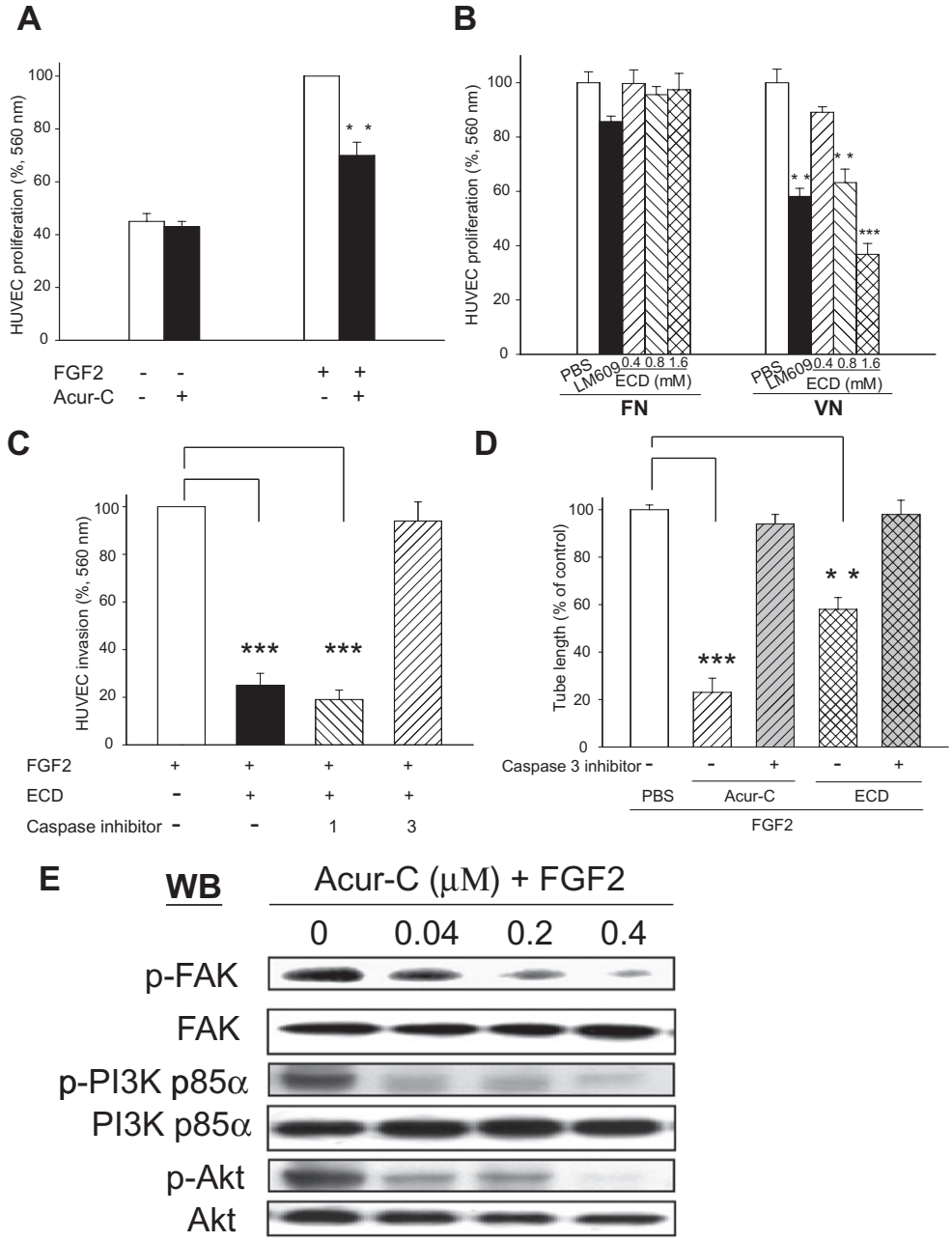

Figure 7 Molecular mechanisms for the inhibition of integrin αvβ3-mediated human umbilical vein endothelial cell (HUVEC) functions by acurhagin-C. (A) HUVECs (10^4 cells per well) in 2% fetal bovine serum (FBS)/M199 were seeded on vitronectin (10 μg·mL^{-1})-coated wells for 2 h attachment. Subsequently, fibroblast growth factor-2 (FGF2) (20 ng·mL^{-1})-containing medium without or with acurhagin-C (Acur-C; 0.4 μM) were added to each well, followed by an additional 12 h incubation. Results are presented as mean ± SEM (n = 4). $^{**}P < 0.01$ as compared with control. (B) HUVECs (10^4 cells per well) in 2% FBS/M199 were plated in fibronectin (FN)- or vitronectin (VN)(10 μg·mL^{-1})-coated wells for attachment. Then, FGF2 (20 ng·mL^{-1})-containing medium without or with LM609 (20 μg·mL^{-1}), or Glu-Cys-Asp (ECD) peptide (0.4, 0.8, 1.6 mM) were added to each well, followed by an additional 24 h incubation. All experiments were performed in quadruplicate and similar results were obtained at least three times. Results are presented as mean ± SEM (n = 4). $^{**}P < 0.01$, $^{***}P < 0.001$, compared with control. (C) Following pretreatment with or without various caspase inhibitors as indicated (50 μM) for 15 min at room temperature, HUVECs (3×10^5 cells per well) were incubated with phosphate-buffered saline (PBS) or ECD peptide (750 μM) in the upper insert chambers and then allowed to invade the Matrigel-coated filter membranes to the lower chambers under the presence of FGF2 (20 ng·mL^{-1}) at 37°C for 24 h. Results are presented as mean ± SEM (n = 4). $^{***}P < 0.001$ as compared with control. (D) The caspase-3 inhibitor suppressed the inhibition by acurhagin-C (Acur-C), as well as ECD peptide (ECD), of the formation of tube-like structures *in vitro*. HUVECs (1×10^5 cells per well) were pretreated without or with a caspase-3 inhibitor (50 μM) for 15 min at room temperature and then co-incubated with PBS, acurhagin-C (0.4 μM) or ECD peptide (750 μM) for additional 15 min. Subsequently, the treated cells were plated on Matrigel-coated wells in the presence of FGF2 (20 ng·mL^{-1}) for 18 h at 37°C. Results are presented as mean ± SEM (n = 4). $^{**}P < 0.01$; $^{***}P < 0.001$ as compared with control. (E) Following serum starvation HUVECs (1×10^6 cells per well) were plated onto culture dishes coated with vitronectin (10 μg·mL^{-1}) and treated with various concentrations of acurhagin-C (Acur-C) before stimulation with FGF2 (20 ng·mL^{-1}) for 30 min and then lysed. Subsequently, HUVEC lysates were applied to 10% SDS-PAGE and Western blotted with the indicated phosphospecific antibodies. After stripping, membranes were reprobed with focal adhesion kinase (FAK)-, phosphatidylinositol 3-kinase (PI3K) p85α- and Akt-specific antibodies as indicated.

Figure 7E, acurhagin-C exerted concentration-dependent inhibition of the phosphorylation of PI3K p85α (Tyr508) and its downstream effector Akt (Ser473). Thus acurhagin-C can substantially disrupt the anchorage-dependent αvβ3/FAK/PI3K/Akt survival signalling in HUVECs.

Discussion

Angiogenesis is an important process for the growth of solid tumours and is partially regulated by adhesion molecules. Activation of integrin αvβ3 may trigger survival signals that promote blood vessel growth and differentiation. Therefore, inhibition of angiogenesis is thought to be a promising strategy in the treatment of tumours. Presently, several lines of evidence show that integrin αvβ3 antagonists are potent angiogenesis inhibitors, and many classes of inhibitors including peptides, antibodies and small organic molecules have been developed (Nicolaou *et al*., 1998; Gutheil *et al*., 2000). In particular, peptides will become the safest and the least toxic therapy for diseases associated with angiogenesis (Nakamura and Matsumoto, 2005). In the present study, acurhagin-C, acting as an antagonist of the integrin αvβ3, inhibited HUVEC behaviours, such as adhesion, motility and differentiation (Figures 1–4 and 7A).

As shown in Figure 7A, acurhagin-C caused a significant inhibition of FGF2-induced HUVEC proliferation at 0.4 μM. This result is consistent with the previous finding of a disintegrin-like protein from *Bothrops alternatus* venom, alternagin-C, that inhibited FGF2-induced proliferation at 0.1 μM (Cominetti *et al*., 2004).

Previously, SVMPs were classified into various protein groups (P-I to P-IV). In general, both classes P-I and P-III can induce HUVEC apoptosis. For P-I SVMPs, suppressing their enzymatic activity can abolish their apoptosis-inducing function. However, halysase, a P-III SVMP, induces endothelial apoptosis without exerting enzymic activity (You *et al*., 2003). Therefore, this result seems to reveal that the disintegrin-like and cysteine-rich domains of P-III SVMPs can promote HUVEC apoptosis by interfering with the cell-ECM interactions. Moreover, the disintegrin-like domain may regulate the catalytic activity of metalloproteinase by modulating the hydrolysis of ECMs, suggesting the effects of P-III SVMPs on cellular functions may involve the interactions of their various domains present in these proteins (Diaz *et al*., 2005).

In the assay of HUVEC adhesion to immobilized ECMs, acurhagin-C markedly inhibited HUVEC adhesion to vitronectin (Figure 2A). Also, acurhagin-C potently reduced FGF2-stimulated endothelial tube formation on Matrigel (Figures 4Ac and 7D) and showed a concentration-dependent inhibition of spontaneous angiogenesis in the ERK-dependent CAM model (Figure 4Bd–f,C). Using FITC-23C6 and FITC-AK7 as primary probes, acurhagin-C was shown to inhibit the binding of 23C6 but not that of AK7 to HUVEC, suggesting acurhagin-C and 23C6 may bind to the same or the overlapped epitope on αvβ3 (Figure 5A). Because triflavin has been identified as a potent angiogenesis inhibitor, the RGD motif of triflavin is a critical recognition sequence in its interaction with endothelial αvβ3 (Sheu *et al*., 1997). However, both acurhagin and acurhagin-C also bound to αvβ3 in a concentration-dependent manner, indicating that the ECD motif in the disintegrin-like domain within acurhagin-C may be crucial for its binding capacity. There are, probably, some motifs other than ECD that contribute to such interaction and these need to be identified. Using the synthetic peptides as tools, our study indicated that the ECD-containing region in the disintegrin-like domain of acurhagin-C was necessary for its inhibitory effect on HUVEC functions. As shown in Figure 7B–D, the ECD peptide derived from acurhagin-C could inhibit FGF2-induced proliferation, invasion and *in vitro* angiogenesis. In fact, this region is the positional homologue of the RGD loop of disintegrin. The two significant differences between the regions of the disintegrin-like domain in acurhagin-C and the RGD loop in triflavin are the XXECD substitution for RGDXX and the presence of an unidentified disulfide bonded cysteinyl residue (*E*CD) in disintegrin-like proteins. Given these differences, it is interesting that acurhagin-C inhibited endothelial behaviours and exhibited a similar potency to that of triflavin, in the interactions of such regions of the disintegrin-like domain with the endothelial αvβ3. Therefore, the structure of the ECD region in the disintegrin-like domain of acurhagin-C appears to be essential for its biological activities, as the synthetic linear ECD peptide lacking disulfide linkages was able to affect endothelial cells.

Previous studies have demonstrated that αvβ3 antagonism can trigger endothelial apoptosis. Brassard *et al*. (1999) proposed that the cell death induced by an RGD disintegrin echistatin binding to αvβ3 results in an apoptotic signal occurring prior to matrix detachment in AvB3–293 cells. Similar results obtained by caspase-3 activation and immunoblotting analyses also strongly suggested that the apoptotic effects observed in acurhagin-C-treated HUVEC relate to the activation of procaspase-3 and inhibition of intracellular signalling, not to detachment-induced apoptosis (Figures 6 and 7). As adhesion of HUVECs to ECMs is an anchorage-dependent process, it is reasonable to expect that failure to adhere to a substratum may generate a signal to activate a suicide cascade in HUVECs. Those data demonstrate that when adhesion is blocked, HUVEC rapidly undergo cell death with the morphological and biochemical characteristics of apoptosis. The round cell shape caused by an altered interaction with ECMs and prevention of cytoskeletal organization represent signals for cell death in HUVECs (Figure 2B). Therefore, it appeared that acurhagin-C, an ECD disintegrin, may induce apoptosis by direct caspase-3 activation. Although Buckley *et al*. (1999) had suggested that RGD-containing peptides can induce apoptosis via triggering a conformational change in procaspase-3 and then promoting procaspase-3 activation, the exact interaction sites involved in the acurhagin-C molecule with procaspase-3 remain to be investigated. Perhaps the ECD peptide, similar to the RGD peptide, can penetrate cell membranes and then induce apoptosis by direct caspase-3 activation through its interaction with a non-RGD-binding site of caspase-3 (Adderley and Fitzgerald, 2000). Thus, the biological activity of ECD peptide might be more versatile than simple disruption of cell adhesion.

Cell adhesion is a critical event in various biological phenomena such as proliferation and differentiation. Integrins on cell surface can mediate cell adhesion by connecting ECMs to intracellular cytoskeleton. With the loss of appropriate

ECMs contacts, cells may undergo apoptosis (Meredith and Schwartz, 1997). However, a possible physiological significance of the integrin-mediated apoptosis is that it may prevent cells from adhering to inappropriate circumstances, because attachment through the incorrect integrin would induce apoptosis (Kumar, 1998). Overall, acurhagin-C competes with ECMs for the binding to αvβ3 on suspended or proliferating endothelial cells and thereafter disrupts focal adhesions, as well as inactivating the FAK/PI3K/Akt survival signalling, leading to endothelial apoptosis through direct procaspase-3 activation and subsequent DNA fragmentation.

In conclusion, therapeutic efforts to target the integrin αvβ3 for the treatment of abnormal angiogenesis already become an intriguing approach and a promising strategy to suppress pro-inflammatory responses and induce cancer regression. Acurhagin-C triggers endothelial anoikis by blockade of αvβ3-mediated cell adhesion and survival, thereby initiating a procaspase-3 apoptotic pathway. Furthermore, the functional study using synthetic peptides as probes demonstrated that the ECD-containing region of disintegrin-like domain of acurhagin-C was responsible for its interactions with HUVEC. Therefore, acurhagin-C and its derivatives may be used as a lead compounds for developing new angiostatic agents. However, further evaluation of the inhibition of pathological angiogenesis in animal models by acurhagin-C is required to extend the applications of acurhagin-C in anti-angiogenic therapy.

Acknowledgements

This work was financially supported by grants from Chang-Gung Medical Research Foundation (CMRPF140021 and 140022) and the National Science Council of Taiwan (NSC 96-2320-B-255-002).

Conflict of interest

The author states no conflict of interest.

References

Adderley SR, Fitzgerald DJ (2000). Glycoprotein IIb/IIIa antagonists induce apoptosis in rat cardiomyocytes by caspase-3 activation. *J Biol Chem* **275**: 5760–5766.

Andrews RK, Berndt MC (1998). Adhesion-dependent signalling and the initiation of haemostasis and thrombosis. *Histol Histopathol* **13**: 837–844.

Aznavooriant S, Stracke ML, Parsons J, McClanahan J, Liotta LA (1996). Integrin αvβ3 mediates chemotatic and haptotactic motility in human melanoma cells through different signaling pathways. *J Biol Chem* **271**: 3247–3254.

Bischoff J (1995). Approaches to studying cell adhesion molecules in angiogenesis. *Trends Cell Biol* **5**: 69–74.

Boudreau NJ, Jones PL (1999). Extracellular matrix and integrin signaling: the shape of things to come. *Biochem J* **339**: 481–488.

Boutahar N, Guignandon A, Vico L, Lafage-Proust MH (2004). Mechanical strain on osteoblasts activates autophosphorylation of focal adhesion kinase and proline-rich tyrosine kinase 2 tyrosine sites involved in ERK activation. *J Biol Chem* **279**: 30588–30599.

Brassard DL, Maxwell E, Malkowski M, Nagabhushan TL, Kumar CC, Armstrong L (1999). Integrin αvβ3-mediated activation of apoptosis. *Exp Cell Res* **251**: 33–45.

Buckley CD, Pilling D, Henriquez NV, Parsonage G, Threlfall K, Scheel-Toellner D *et al*. (1999). RGD peptides induce apoptosis by direct caspase-3 activation. *Nature* **397**: 534–539.

Colman RW, Jameson BA, Lin Y, Johnson D, Mousa SA (2000). Domain 5 of high molecular weight kininogen (kininostatin) down-regulates endothelial cell proliferation and migration and inhibits angiogenesis. *Blood* **95**: 543–550.

Cominetti MR, Terruggi CHB, Ramos OHP, Fox JW, Mariano-Oliveira A, De Freitas MS *et al*. (2004). Alternagin-C, a disintegrin-like protein, induces vascular endothelial cell growth factor (VEGF) expression and endothelial cell proliferation *in vitro*. *J Biol Chem* **279**: 18247–18255.

Danen EHJ (2005). Integrins: regulators of tissue function and cancer progression. *Curr Pharm Design* **11**: 881–891.

Diaz C, Valverde L, Brenes O, Rucavado A, Gutierrez JM (2005). Characterization of events associated with apoptosis/anoikis induced by snake venom metalloproteinase BaP1 on human endothelial cells. *J Cell Biochem* **94**: 520–528.

Erdreich-Epstein A, Tran LB, Cox OT, Huang EY, Laug WE, Shimada H *et al*. (2005). Endothelial apoptosis induced by inhibition of integrins αvβ3 and αvβ5 involves ceramide metabolic pathways. *Blood* **105**: 4353–4361.

Frangie C, Zhang WH, Perez J, Xu Dubois YC, Haymann JP, Baud L (2006). Extracellular calpains increase tubular epithelial cell mobility. *J Biol Chem* **281**: 26624–16632.

Friedlander M, Brooks PC, Shaffer RW, Kincaid CM, Varner JA, Cheresh DA (1995). Definition of two angiogenic pathways by distinct αv integrins. *Science* **270**: 1500–1502.

Grossmann J (2002). Molecular mechanisms of 'detachment-induced apoptosis-anoikis'. *Apoptosis* **7**: 247–260.

Gutheil JC, Campbell TN, Pierce PR, Watkins JD, Huse WD, Bodkin DJ *et al*. (2000). Targeted antiangiogenic therapy for cancer using vitaxin: a humanized monoclonal antibody to the integrin αvβ3. *Clin Cancer Res* **6**: 3056–3061.

Gutierrez JM, Rucavado A (2000). Snake venom metalloproteinases: their role in the pathogenesis of local tissue damage. *Biochimie* **82**: 841–850.

Kamiguti AS, Hay CRM, Zuzel M (1996). Inhibition of collagen-induced platelet aggregation as the result of cleavage of α2β1-integrin by the snake venom metalloproteinase jararhagin. *Biochem J* **320**: 635–641.

Kumar CC (1998). Signaling by integrin receptors. *Oncogene* **17**: 1365–1373.

Laing GD, Moura-da-Silva AM (2005). Jararhagin and its multiple effects on hemostasis. *Toxicon* **45**: 987–996.

Marcinkiewicz C (2005). Functional characteristic of snake venom disintegrins: potential therapeutic implication. *Curr Pharm Design* **11**: 815–827.

Meredith JE, Schwartz MA (1997). Integrins, adhesion and apoptosis. *Trends Cell Biol* **7**: 146–150.

Michel JB (2003). Anoikis in the cardiovascular system: known and unknown extracellular mediators. *Arterioscler Thromb Vasc Biol* **23**: 2146–2154.

Mousa SA, Mohamed S (2004). Inhibition of endothelial cell tube formation by the low molecular weight heparin, tinzaparin, is mediated by tissue factor pathway inhibitor. *Thromb Haemost* **92**: 627–633.

Nakamura T, Matsumoto K (2005). Angiogenesis inhibitors: from laboratory to clinical application. *Biochem Biophys Res Commun* **333**: 289–291.

Nicolaou KC, Trujillo JI, Jandeleit B, Chibale K, Rosenfeld M, Diefen-

bach B *et al*. (1998). Design, synthesis and biological evaluation of nonpeptide integrin antagonists. *Bioorg Med Chem* **6**: 1185–1208.

Oliver MH, Harrison NK, Bishop JE, Cole PJ, Laurent GJ (1989). A rapid and convenient assay for counting cells cultured in microwell plates: application for assessment of growth factors. *J Cell Sci* **92**: 513–518.

Ramos OHP, Selistre-de-Araujo HS (2006). Snake venom metalloproteases-structure and function of catalytic and disintegrin domains. *Comp Biochem Physiol C Toxicol Pharmacol* **142**: 328–346.

Sheu JR, Yen MH, Kan YC, Hung WC, Chang PT, Luk HN (1997). Inhibition of angiogenesis *in vitro* and *in vivo*: comparison of the relative activities of triflavin, an Arg-Gly-Asp-containing peptide and anti-αvβ3 integrin monoclonal antibody. *Biochim Biophys Acta* **1336**: 445–454.

Shimokawa K, Shannon JD, Jia L-G, Fox JW (1997). Sequence and biological activity of catrocollastatin-C: a disintegrin-like/cysteine-rich two-domain protein from *Crotalus atrox* venom. *Arch Biochem Biophys* **1997**: 35–43.

Stromblad S, Cheresh D (1996). Cell adhesion and angiogenesis. *Trends Cell Biol* **6**: 462–468.

Tabruyn SP, Sorlet CM, Rentier-Delrue F, Bours V, Weiner RI, Martial JA *et al*. (2003). The antiangiogenic factor 16K human prolactin induces caspase-dependent apoptosis by a mechanism that requires activation of nuclear factor-κB. *Mol Endocrinol* **17**: 1815–1823.

Takahashi R, Sekine N, Nakatakev T (1999). Influence monoclonal antiplatelet glycoprotein antibodies on *in vitro* human megakaryocyte colony formation and proplatelet formation. *Blood* **93**: 1951–1958.

Tan L, Kowalska MA, Romo GM, Lopez JA, Darzynkiewicz Z, Niewiarowski S. (1999). Identification and characterization of endothelial glycoprotein Ib using viper venom proteins modulating cell adhesion. *Blood* **93**: 2605–2616.

Tanjoni I, Weinlich R, Della-Casa MS, Clissa PB, Saldanha-Gama RF, de Freitas MS *et al*. (2005). Jararhagin, a snake venom metalloproteinase, induces a specialized form of apoptosis (anoikis) selective to endothelial cells. *Apoptosis* **10**: 851–861.

Wang WJ (2008). Agglucetin, a tetrameric C-type lectin like venom protein, regulates endothelial cell survival and promotes angiogenesis by activating integrin αvβ3 signaling. *Biochem Biophys Res Commun* **369**: 753–760.

Wang WJ, Huang TF (2002). Purification and characterization of a novel metalloproteinase, acurhagin, from *Agkistrodon acutus* venom. *Thromb Haemost* **87**: 641–650.

Wang WJ, Shih CH, Huang TF (2005). Primary structure and antiplatelet mechanism of a snake venom metalloproteinase, acurhagin, from *Agkistrodon acutus* venom. *Biochimie* **87**: 1065–1077.

Yeh CH, Wang WC, Hsieh TT, Huang TF (2000). Agkistin, a snake venom-derived glycoprotein Ib antagonist, disrupts von Willebrand factor-endothelial cell interaction and inhibits angiogenesis. *J Biol Chem* **275**: 18615–18618.

You WK, Seo HJ, Chung KH, Kim DS (2003). A novel metalloprotease from *Gloydius halys* venom induces endothelial cell apoptosis through its protease and disintegrin-like domains. *J Biochem* **134**: 739–749.